Strain effects on the phonon thermal properties of ultra-scaled Si nanowires

Abhijeet Paul[a] and Gerhard Klimeck
School of Electrical and Computer Engineering, Network for Computational Nanotechnology, Purdue University, West Lafayette, Indiana 47907, USA

(Received 5 May 2011; accepted 8 August 2011; published online 26 August 2011)

The impact of uniaxial and hydrostatic stress on the ballistic thermal conductance (κ_l) and the specific heat (C_v) of [100] and [110] Si nanowires are explored using a Modified Valence Force Field phonon model. An anisotropic behavior of κ_l and isotropic nature of C_v under strain are predicted for the two wire orientations. Compressive (tensile) strain decreases (increases) C_v. The C_v trend with strain is controlled by the high energy phonon sub-bands. Dominant contribution of the low/mid (low/high) energy bands in [100] ([110]) wire and their variation under strain governs the behavior of κ_l. © *2011 American Institute of Physics*. [doi:10.1063/1.3630228]

The wide application of silicon nanowires (SiNWs) in areas ranging from complementary-metal-oxide-semiconductor transistors[1,2] to thermoelectric (TE) devices,[3] non-volatile memories,[4] and solar cells[5] has made SiNWs an extremely useful nano-electronics device concept. Device properties can be engineered[6,7] through the introduction of built-in stress by process engineering and by external forces like wafer bending.[8] Tuning lattice thermal properties using strain can be beneficial for cooling and increasing gain of lasers[8,9] or improving the efficiency of TE devices.[9]

Prior work: Strain/stress effects on the thermal conductivity of doped bulk zinc-blende (ZB) semiconductors at low temperatures has been well studied.[10,11] Most of the bulk studies in ZB semiconductors found decrease in thermal conductivity with tensile strain which is qualitatively attributed to (1) a decrease in the phonon mean free path,[12] (2) an increase in the Debye temperature,[8,12] and (3) a change in the material stiffness.[13] The few experimental[14] and theoretical[8,9,13,15] efforts that have focused on the strain effects on the thermal properties in nanostructures are either limited to single crystal orientation (mostly [100]) or diffusive phonon transport even in small nanostructures. This work investigates the external strain effects on the thermal properties in ultra-scaled SiNWs in the coherent phonon transport regime where the wire cross-section sizes are comparable to the phonon wavelengths[16] ($\lambda_{ph} = hV_{snd}/k_BT_{300K} \approx 1$ nm at $V_{snd} = 6.5$ km/s for a 3 nm × 3 nm [100] SiNW,[17] where k_B and h are the Boltzmann constant and Planck's constant, respectively). The thermal properties in this work refer to the phonon dominated lattice properties. The correlation of the thermal properties to the electronic properties are not addressed as they are outside the scope of the present work.

Free-standing SiNWs' phonon dispersion are studied using the modified valence force (MVFF) model.[17–19] The MVFF model has been shown to correctly reproduce the strain effects like the Gruneisen parameters[18,19] and third order elastic constants in bulk Si and Ge.[18] The same set of Si MVFF parameters[18,19] are used in this work to model the SiNW phonon dispersion under hydrostatic and uniaxial stress.

The ballistic thermal conductance (κ_l) across a semiconductor wire maintained under a small temperature gradient ΔT can be calculated from the calculated phonon dispersion, using the Landauer's formula[20] using Eq. (1),[21,22]

$$\kappa_l(\epsilon, T) = \frac{e^2}{\hbar} \sum_{i \in [1,N]} \kappa_l^i(\epsilon, T), \tag{1}$$

where

$$\kappa_l^i(\epsilon, T) = \int_{E_{i,min}}^{E_{i,max}} M(\epsilon, E_i) \cdot E_i \cdot \frac{\partial}{\partial T} \left[\frac{1}{\left(exp\left(\frac{E_i}{k_BT}\right) - 1\right)} \right] dE_i, \tag{2}$$

where N is the number of energy bins in the entire phonon dispersion energy range. The terms ϵ, M(E), T, and e are the strain percentage, the number of modes at phonon energy E, the temperature, and the electronic charge, respectively. The term $\kappa_l^i(E,T)$ is the contribution to the total κ_l of SiNW for $E_{i,min} \leq E < E_{i,max}$. This energy resolved representation in Eq. (1) allows for better understanding of the variation in κ_l due to strain.

From the calculated phonon dispersion, the constant volume specific heat (C_v) at a given T can be calculated[23] as

$$C_v(T) = \left(\frac{k_B}{m_{uc}}\right) \cdot \sum_{n,q} \left[\frac{\left(\frac{E_{n,q}}{k_BT}\right) \cdot exp\left(\frac{-E_{n,q}}{k_BT}\right)}{\left[1 - exp\left(\frac{-E_{n,q}}{k_BT}\right)\right]^2} \right] \quad [\mathrm{J/kgK}], \tag{3}$$

where m_{uc} is the mass of the SiNW unitcell in kg. The quantity $E_{n,q}$ is the phonon eigen energy associated with the branch "n" and crystal momentum vector "q".

SiNW details: Square NWs with width (W) and height (H) = 3 nm with two channel orientations of [100] and [110] are studied (inset of Figs. 1(a) and 1(b)). Hydrostatic deformation (equal deformation along all the directions) and uniaxial deformation (along the wire axis) are applied to these wires varying up to ±2%. The outer surface atoms in these NWs are allowed to vibrate freely. Extremely small SiNWs may show significant surface and internal atomic reconstruction[9,24] or phase change[9] under strain leading to larger changes in C_v and κ_l, which are outside the scope of the present study.

[a]Electronic mail: abhijeet.rama@gmail.com.

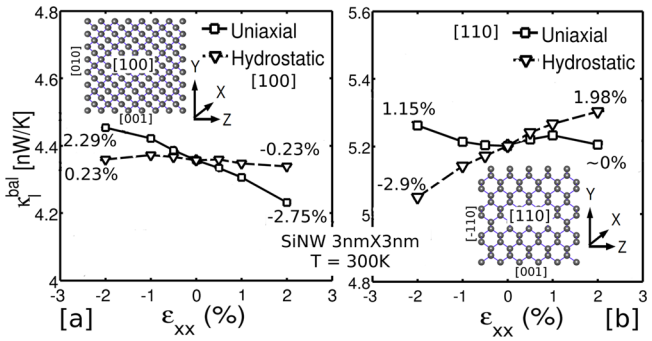

FIG. 1. (Color online) Variation in κ_l with hydrostatic and uniaxial stress in 3 nm × 3 nm SiNW with (a) [100] and (b) [110] orientations. The uniaxial stress is applied along the wire axis. Insets also show the atomic structures of both the SiNWs with the coordinate axes.

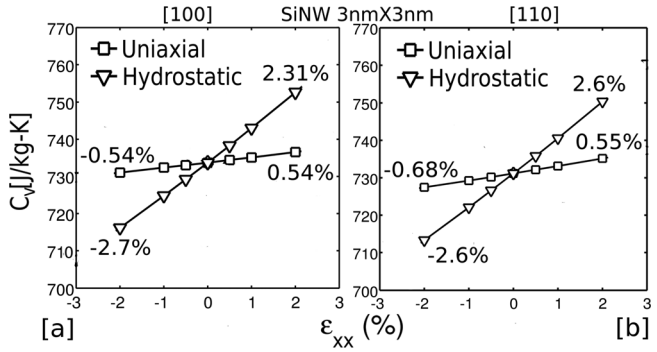

FIG. 2. Variation in the C_v with stress in 3 nm × 3 nm SiNW with (a) [100] and (b) [110] orientations. Two types of stress are applied in these SiNWs: (1) hydrostatic pressure and (2) uniaxial stress along the wire axis.

Ballistic thermal conductance κ_l*:* In all the SiNWs, κ_l is calculated using Eq. (1) at 300 K. κ_l increases (decreases) under uniaxial compression (tension) for both the wire orientations. Similar variations in κ_l for [100] SiNWs are also observed by Li *et al.*[9] using non-equilibrium molecular dynamics calculations. The [100] SiNW shows larger variation in κ_l under tensile uniaxial deformation compared to the [110] SiNW (Figs. 1(a) and 1(b)). κ_l shows a weak hydrostatic stress dependence in [100] SiNW in contrast to the [110] SiNW which shows a decrease (increase) of 2.9% (1.98%) in κ_l under 2% compressive (tensile) strain from the unstrained value (Figs. 1(a) and 1(b)). *Thus, ultra-scaled SiNWs show an anisotropic variation in* κ_l *under hydrostatic deformation.*

Specific heat (C_v)*:* Variation in the phonon dispersion under strain also changes the C_v of SiNWs. Compressive (tensile) strain decreases (increases) the C_v in both types of SiNWs (Figs. 2(a) and 2(b)). This variation in C_v is similar to the bulk Si behavior as reported in Refs. 13 and 15. Under hydrostatic stress, the C_v decreases by ≈2.7% at 2% compression and increases to ≈2.6% at 2% expansion compared to the unstrained C_v value for both the SiNW orientations. Under uniaxial deformation, the variation is ≤1% for ±2% strain for both wire orientations (Figs. 2(a) and 2(b)). *Hence, C_v variation is isotropic under strain in ultra-scaled SiNWs.*

Reason for the variation in κ_l*:* To understand the variation in κ_l with strain, the energy dependent contributions are analyzed using Eq. (1). The entire phonon spectrum is grouped into three energy ranges: (1) E_L ("low" bands), (2) E_M ("mid" bands), and (3) E_H ("high" bands) (see Fig. 3(a)). These bands show variable contributions under strain which determine the overall effect on κ_l (Table I).

Under uniaxial strain, in [100] SiNW, the contribution to κ_l is mainly from $E_L + E_M$, which decreases from ~88% under compression (Cm) to ~84% under tension (Tn) (Fig. 3(b)), whereas in [110] SiNW, the contribution to κ_l is mainly from $E_L + E_H$, which reduces from ~59% (Cm) to ~54% (Tn) (Fig. 3(d)). Under hydrostatic strain, in [100] SiNW, main contribution to κ_l is from E_M, which reduces from ~56% (Cm) to ~45% (Tn) (Fig. 3(c)), while in [110] SiNW, main contribution to κ_l is from $E_L + E_H$, which

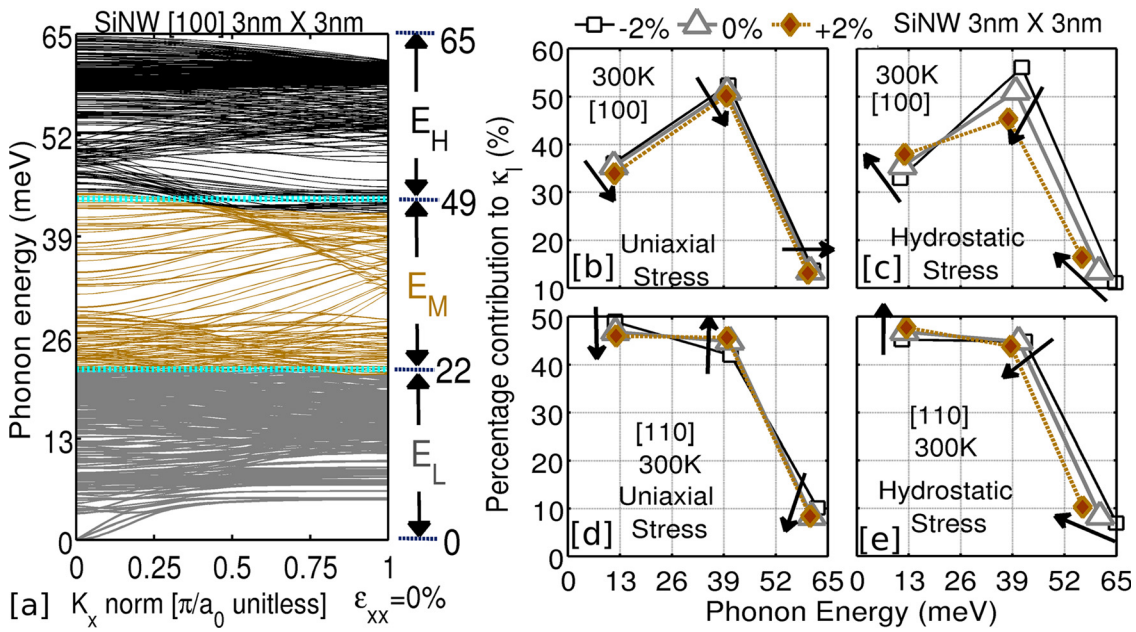

FIG. 3. (Color online) (a) Phonon dispersion of 3 nm × 3 nm [100] SiNW with the three energy ranges considered for κ_l analysis. The percentage contribution to κ_l from different energy ranges, for [100] SiNW under (b) uniaxial stress, (c) hydrostatic stress, and for [110] SiNW under (d) uniaxial stress and (e) hydrostatic stress. Arrows show the variation in contribution from compression (Cm) to tension (Tn).

TABLE I. Value of band contribution to κ_l under strain (Fig. 3). Variation shown from compression (Cm) to tension (Tn) for uniaxial (Un) and hydrostatic (Hy) strain for both SiNW orientations (Or).

Strain, [Or] E_i (meV) →	$\kappa_l(L)$ (0-22)	$\kappa_l(M)$ (22-44)	$\kappa_l(H)$ (44-65)	Dominant band	Cm to Tn
Un, [100]	36%–34% ↓	52%–50% ↓	13%–13%	L,M	↓
Hy, [100]	32%–37% ↑	56%–45% ↓	11%–16% ↑	M	↓
Un, [110]	49%–46% ↓	42%–46% ↑	10%–8% ↓	L,H	↓
Hy, [110]	45%–48% ↑	45%–44% ↓	7%–10% ↑	L,H	↑

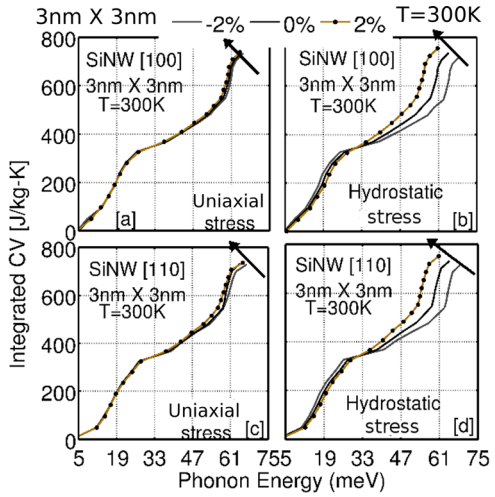

FIG. 4. (Color online) Variation in CV with phonon energy bands under various conditions. 3 nm × 3 nm [100] SiNW with (a) uniaxial stress, (b) hydrostatic pressure. 3 nm × 3 nm [110] SiNW with (c) uniaxial stress, (d) hydrostatic pressure. The higher sub-bands show larger variation in CV contribution compared to the lower energy sub-bands.

increases from ~52% (Cm) to ~58% (Fig. 3(e)). These details are also summarized in Table I. *Thus, low/mid energy contribution for [100] SiNW and low/high energy contribution for [110] SiNW explains the anisotropic nature of* κ_l.

Reason for C_v *variation:* Under the action of strain the contribution of the phonon bands in E_H range varies considerably as shown in Fig. 4. Under uniaxial stress, both [100] and [110] SiNWs show almost no variation in the E_L and E_M range and minute variation in the E_H range(Figs. 4(a) and 4(c)). The contribution increases from Cm to Tn in the E_H range which governs the C_v trend under uniaxial strain (Fig. 2). Under hydrostatic stress, contribution from the E_H range increases from Cm to Tn, but in a much larger magnitude compared to uniaxial stress, for both the wire orientations (Figs. 4(b) and 4(d)). This explains the larger variation in C_v under hydrostatic stress (Fig. 2). *Thus, the higher energy bands decide the strain behavior of* C_v *under strain, for ultra-scaled SiNWs.*

Conclusions and outlook: The impact of strain on the thermal properties of ultra-scaled SiNWs has been provided. The ballistic thermal conductance behaves an-isotropically under strain; however, C_v shows an isotropic behavior. Similar strain behavior for lattice thermal properties are obtained in SiNWs with W = H up to 6 nm, which are not shown for the sake of brevity. The observed trends in the lattice thermal properties can be understood by the different types of contribution of phonon modes in different energy ranges. The behavior of C_v in SiNWs is similar to bulk Si; however, κ_l variation is very different from bulk Si. Under the low stress condition, hydrostatic strain can be beneficial in engineering C_v and uniaxial stress for engineering κ_l for cooling lasers. However, high external strain ($|\epsilon| > 2\%$) field may be needed to engineer κ_l to improve the efficiency of TE devices.[25] The presence of surface roughness, phonon-phonon and phonon-electron scattering may reduce the values of κ_l; however, the trend with strain is expected to remain the same.

The authors acknowledge financial support from MSD and FCRP under SRC, NRI under MIND, NSF, and Purdue University, and computational support from nanoHUB.org, an NCN operated and NSF funded project.

[1]N. Singh, A. Agarwal, L. K. Bera, T. Y. Liow, R. Yang, S. C. Rustagi, C. H. Tung, R. Kumar, G. Q. Lo, N. Balasubramanian, and D. L. Kwong, IEEE Electron Device Lett. **27**, 383 (2006).
[2]K. H. Yeo, S. D. Suk, M. Li, Y. Y. Teoh, K. H. Cho, K. H. Hong, S. K. Yun, M. S. Lee, N. M. Cho, K. H. Lee, D. Y. Hwang, B. K. Park, D. W. Kim, D. G. Park, and B. I. Ryu, IEEE IEDM Tech. Dig. **2006**, 539.
[3]A. I. Hochbaum, R. Chen, R. D. Delgado, W. Liang, E. C. Garnett, M. Najarian, A. Majumdar, and P. Yang, Nature (London) **451**, 163 (2008).
[4]Q. Li, X. Zhu, H. D. Xiong, S.-M. Koo, D. E. Ioannou, J. J. Kopanski, J. S. Suehle, and C. A. Richter, Nanotechnology **18**, 235204 (2007).
[5]E. Garnett and P. Yang, Nano Lett. **10**, 1082 (2010).
[6]P. Hashemi, L. Gomez, M. Canonico, and J. Hoyt, Tech. Dig. - Int. Electron Devices Meet. **2008**, 1.
[7]O. Bonno, S. Barraud, D. Mariolle, and F. Andrieu, J. Appl. Phys. **103**, 063715 (2008).
[8]R. C. Picu, T. Borca-Tasciuc, and M. C. Pavel, J. Appl. Phys. **93**, 3535 (2003).
[9]X. Li, K. Maute, M. L. Dunn, and R. Yang, Phys. Rev. B **81**, 245318 (2010).
[10]K. C. Sood and M. K. Roy, Phys. Rev. B **46**, 7486 (1992).
[11]A. Ramdane, B. Salce, and L. J. Challis, Phys. Rev. B **27**, 2554 (1983).
[12]M. Roufosse and P. G. Klemens, Phys. Rev. B **7**, 5379 (1973).
[13]Y. Xu and G. Li, J. Appl. Phys. **106**, 114302 (2009).
[14]T. Borca, W. Liu, J. Liu, T. Zeng, D. W. Song, C. D. Moore, G. Chen, K. L. Wang, and M. S. Goorsky, Superlattices Microstruct. **28**, 199 (2000).
[15]H. Zhao, Z. Tang, G. Li, and N. R. Aluru, J. Appl. Phys. **99**, 064314 (2006).
[16]C. Dames and G. Chen, J. Appl. Phys. **95**, 682 (2004).
[17]A. Paul, M. Luisier, and G. Klimeck, *14th Int. Workshop on Compt. Elect.* (IWCE, Pisa, Italy, 2010).
[18]Z. Sui and I. P. Herman, Phys. Rev. B **48**, 17938 (1993).
[19]A. Paul, M. Luisier, and G. Klimeck, J. Comput. Electron. **9**, 160 (2010).
[20]R. Landauer, IBM J. Res. Dev. **1**, 223 (1957).
[21]T. Markussen, A.-P. Jauho, and M. Brandbyge, Nano Lett. **8**, 3771 (2008).
[22]N. Mingo, L. Yang, D. Li, and A. Majumdar, Nano Lett. **3**, 1713 (2003).
[23]D. C. Wallace, *Thermodynamics of Crystals* (Dover, NewYork, 1998), p. 190.
[24]A. Palaria, G. Klimeck, and A. Strachan, Phys. Rev. B **78**, 205315 (2008).
[25]W. Zhang, T. S. Fisher, ASME Conf. Proc. **2005**, 683 (2005).